Stability Limit of Electrified Droplets

J. Beroz, A. J. Hart, and J. W. M. Bush

Phys. Rev. Lett. **122**, 244501 — Published 17 June 2019

DOI: 10.1103/PhysRevLett.122.244501

Title: The Stability Limit of Electrified Droplets

Authors: J. Beroz[1,2*], A. J. Hart[2], J. W. M. Bush[3]

Affiliations:

[1]Department of Physics, Massachusetts Institute of Technology, Cambridge, MA 02139, USA.

[2]Department of Mechanical Engineering, Massachusetts Institute of Technology, Cambridge, MA 02139, USA

[3]Department of Applied Mathematics, Massachusetts Institute of Technology, Cambridge, MA 02139, USA

*Correspondence to: jberoz@mit.edu

Received date: 1/5/2019

Abstract: In many physical processes, including cloud electrification, electrospray and demulsification, droplets and bubbles are exposed to electric fields and may either remain whole or burst in response to electrical stresses. Determining the stability limit of a droplet exposed to an external electric field has been a longstanding mathematical challenge, and the only analytical treatment to date is an approximate calculation for the particular case of a free floating droplet. Here we demonstrate, experimentally and theoretically, that the stability limit of a conducting droplet or bubble exposed to an external electric field is described by a power law with broad generality, that, in practice, applies to the cases in which the droplet or bubble is pinned or sliding on a conducting surface, or free floating. This power law can facilitate the design of devices for liquid manipulation via a simple formula that captures the parameter range of bubbles and droplets that can be supported on electrified surfaces.

Main Text: A liquid droplet will typically deform when subject to an electric field, owing to the generation of electrical stresses at its surface. For sufficiently strong electric fields, the drop may become mechanically unstable and emit charged microscopic liquid jets [1,2]. A laboratory curiosity a century ago [3,4], the electrical stability limit of droplets was first recognized to be of meteorological importance, for example in determining the size of water droplets in thunderstorms and creating preferred conduction paths for lightning strikes [5,6]. The stability limit of a conductive free floating droplet in a uniform electric field was first determined by G.I. Taylor by a combination of experiment and dimensional analysis (Fig. 2b(i)) [7], and later by an approximate calculation wherein the deformed shape of the droplet was assumed spheroidal [1].

Further investigations of the stability of electrified droplets and the dynamic process of jet emission [1,2,8] provided the conceptual basis for several important technologies. These include electrospraying, wherein a liquid confined at the orifice of a nozzle is electrified above its stability limit in order to controllably produce fine liquid droplets or ionized mists [9]. This technique underlies methods of high-resolution printing [10], mass spectrometry [11], ion beam generation [12], air purification [13], and space propulsion [14]. Similarly, electrospinning involves ejecting fine liquid filaments from electrified droplets [15] for manufacture of fibers for filters [16], composite materials [17], nanogenerators [18], tissue scaffolds [19], and drug delivery devices [20]. Careful application of an electric field below the droplet stability limit is also used to control mixing and coalescence of emulsion droplets [21,22].

Despite longstanding scientific and practical interest, an analytical representation for the stability limit of electrified droplets has not been derived for the simplest general case, namely, that of a conducting drop on a conducting surface exposed to a uniform external field in a dielectric medium (Fig. 1). The particular case where the droplet's surface intersects the conducting surface at a right angle corresponds to half of a free floating droplet in a uniform electric field. In the absence of an analytical treatment, numerical computations have been performed [23–26] and engineering development often involves semi-empirical formulas and trial-and-error [11–14,16,17,19,22].

The difficulty in modelling the droplet's stability arises from the fact that the droplet's critically stable shape, i.e., the limiting static shape just prior to bursting through the rapid formation of a jet (Fig. S1), does not appear to be elementary, and the family of critically stable shapes found by varying parameters exhibits no apparent similarity (Fig. 2a). These shapes are also quite different from the spherical shape the droplet would assume in the absence of the electric field. Moreover, the configuration of the electric field, the shape of the droplet, and the liquid pressure inside the droplet are coupled, which requires all to be solved for simultaneously, unlike solving for the shape of a droplet in a gravitational [27] or centrifugal field [28]. Mathematically, this problem poses a set of coupled nonlinear partial differential equations where the solution must satisfy the balance of electrostatic, surface tension, and internal liquid pressures normal to the droplet's equipotential surface [24]. These pressures are all conservative, so an equivalent formulation is to find the free energy minimum from an integrated form of the coupled nonlinear differential equations [29]. In neither case does a known closed-form solution exist. Here we show that, provided the effect of gravity is negligible, the stability limit for a conducting droplet on a conducting surface follows a power law, simply derivable by the variational principle, that is in excellent agreement with our experiments (Fig. 2b). The power law captures the cases for which droplets or bubbles are either pinned or sliding on the conducting surface, or free floating.

Our experiment apparatus comprises a metal plate with a circular hole machined through the center, within which resides a metal needle with its tip coincident with the plate's surface (Fig. 1). For each experiment, the plate and needle are electrically grounded, and a second parallel plate is situated above and held at a different constant electrical potential. The dimensions and separation distance between the plates are such that a uniform far field E_0 is established [30]. Soapy water (surface tension $\gamma = 0.029\,\mathrm{N/m}$) is slowly dispensed through the needle by a motorized syringe, which establishes and feeds a droplet confined to the outer radius *R* of the needle tip by a small air gap of negligible dimension between the needle and plate. A high-speed camera records the droplet as it quasi-statically increases in volume and then becomes unstable (Fig. S1). The droplet behaves as a conductor because the timescale for cancellation of the electric field inside the droplet is much smaller than the timescale for filling the droplet over the course of the experiments. Specifically, the timescale for filling the droplet is $\sim 10^1$ sec, and the timescale for electrical relaxation is $\tau_E = \varepsilon_l / \sigma_l \lesssim 1.3\times10^{-4}$ sec [31], where $\varepsilon_l \approx 80\varepsilon_0$ and $\sigma_l \approx 5.6\times10^{-6}$ S/m are the permittivity and conductivity of the soapy water, and $\varepsilon_0 = 8.85\times10^{-12}\,\mathrm{F/m}$ is the vacuum permittivity. Note that ambient air surrounds the droplets, so $\varepsilon \approx \varepsilon_0$. At these fill rates, the dynamic fluid pressures inside the droplet are negligible (see SI). The video frame containing the critically stable droplet shape is image processed to calculate relevant quantities, specifically the droplet's volume *V*, apex height *H* and contact angle *θ* (Fig. 1).

The full range of experimental data was acquired by systematically changing E_0 for two needle radii $R = [0.46, 0.74]\,\mathrm{mm}$ in order to work within two experimental constraints: (1) avoiding electrical breakdown of the air which limits E_0; and (2) requiring the effect of gravity to be negligible, i.e., the Bond number $\rho g V^{2/3}/\gamma \lesssim 0.1$, where the soapy water density $\rho \approx 10^3\,\mathrm{kg/m^3}$, and the gravitational acceleration $g = 9.8\,\mathrm{m/s^2}$. Practically, this meant that R could not exceed ~1mm, otherwise, gravity would become significant [32]. The range of the experimental results was ultimately limited by the electrified droplets depinning from the edge of the needle before becoming unstable at $\theta \approx 0$ and $\theta \approx \pi/2$.

For each experiment, the stability limit is fully specified by γ, εE_0^2 and two geometric parameters that define the droplet shape; specifically we choose the droplet volume V and radius R. This set of parameters comprises two dimensionless groups which are functionally related according to the Buckingham Pi theorem [33] : $\dfrac{\varepsilon E_0^2}{\gamma/R}$, a ratio of characteristic electrostatic and capillary pressures (i.e. the electrical Bond number), and $\dfrac{R^3}{V}$, a shape parameter. The absolute length scale of the experiment enters only through the dimensionless group $\dfrac{\varepsilon E_0^2}{\gamma/R}$ through R; thus, it is natural to choose R as the unit scale of the coordinate axes for displaying the family of critically stable droplet shapes (Fig. 2a).

We proceed by demonstrating that these two dimensionless groups must be proportional to one another. The quasi-static droplet shapes observed during experiments all correspond to minima of the free energy *F*, i.e., $dF = 0$, and the critically stable droplet shapes are the limiting case at which $dF = 0$. Let an arbitrary variation about some particular critically stable droplet shape be parameterized by the dimensionless parameter ξ, where the critically stable shape is $\xi = \xi_0$. Only variations at constant volume are physical and the experiment is performed at constant ambient temperature. Therefore there are only two nonzero terms comprising dF, specifically the differential changes in surface energy $dU_\gamma(\xi)$ and electrostatic energy $dU_E(\xi)$ due to the variation. Hence $dF = \left(U'_\gamma(\xi_0) + U'_E(\xi_0)\right) d\xi = 0$, or equivalently $U'_\gamma(\xi_0) + U'_E(\xi_0) = 0$ because the variation $d\xi$ is arbitrary; the prime superscript denotes a partial derivative with respect to ξ.

The surface energy of the droplet may be written as $U_\gamma(\xi) = \gamma R^2 a(\xi)$, where $R^2 a(\xi)$ is the droplet's surface area and $a(\xi)$ is a dimensionless shape function. The energy of the electrostatic field due to the presence of the droplet may be written as $U_E(\xi) = \varepsilon E_0^2 V \upsilon(\xi)$, where similarly $\upsilon(\xi)$ is a dimensionless shape function. The scaling intuition for $U_E(\xi)$ is that the uniform far field E_0 sets the scale of the energy density everywhere to be εE_0^2, and the relevant cubic length scale is V. However, it is important to bear in mind that the electrostatic field at the surface of the droplet has a complicated relationship to E_0 due to of the coupling between the droplet shape and electric field configuration (see SI). More precisely, $U_E(\xi)$ is the difference between the electrostatic energy of the field surrounding the droplet and that of the spatially homogeneous field E_0 that would exist in the droplet's absence (i.e. for $V \equiv 0$). The same expression for

$U_E(\xi)$ is also found by considering the polarization energy of the free floating shape in the uniform electric field E_0 defined by the equipotential surface comprised of the critically stable droplet's surface and the surface of the metal plate (see SI). An explicit expression for $\upsilon(\xi)$ generally involves an infinite series of Legendre functions found by solving an eigenvalue problem constructed for the critically stable shape $\xi = \xi_0$ [34,35]. The coefficients multiplying each term in the infinite series must conspire such that V simply multiplies $\upsilon(\xi)$, and it is assumed that $U_E(\xi)$ includes the energy spent transferring charge to the surface of droplet and metal plate so that the electrical potential remains constant.

The variation about $dF = 0$ therefore becomes $\varepsilon E_0^2 V \upsilon'(\xi_0) + \gamma R^2 a'(\xi_0) = 0$, or equivalently $\left(\frac{\varepsilon E_0^2}{\gamma/R}\right)^{-1} \frac{R^3}{V} = -\frac{\upsilon'(\xi_0)}{a'(\xi_0)}$. Again, because the variation is arbitrary, we may infer that $-\frac{\upsilon'(\xi_0)}{a'(\xi_0)} = c$, where c a positive dimensionless coefficient. Substituting and rearranging yields the power law for the critically stable droplet shapes $\frac{R^3}{V} = c\frac{\varepsilon E_0^2}{\gamma/R}$. Fitting to experiment yields the proportionality constant $c \approx \pi/2$ (Fig. 2b) and therefore

$$\frac{R^3}{V} = \frac{\pi}{2}\frac{\varepsilon E_0^2}{\gamma/R}. \tag{1}$$

The geometric parameters V and R are special choices because they are the only two geometric parameters that are constant with respect to the variation. The power law results from the substitution $\upsilon'(\xi_0) = -ca'(\xi_0)$ above, which removes the complicated details of the critically stable droplet shapes that reside in $a(\xi_0)$ and $\upsilon(\xi_0)$. For this reason, we expect Eq. 1 to remain valid for the critically stable droplet shapes with $\theta \gtrsim \pi/2$, which were beyond our experimental capabilities. From a dimensional analysis point of view, *V* and *R* are not unique choices and may be exchanged for any two geometric parameters that define the droplet shape. Historically, the choices have been *H* and *R* [1,7,8,23,24], which yield the dimensionless groups $\frac{\varepsilon E_0^2}{\gamma/R}$ and $\frac{R}{H}$. However, *H* is not constant with respect to the variation and therefore the above derivation cannot be repeated to arrive at an analogous power law. Essentially, the complicated details of the critically stable droplet shapes reside within *H*, which precludes a power law between these dimensionless groups (Fig. S2). This discussion illustrates the importance of our choice of the governing parameter set $\left[\gamma, \varepsilon E_0^2, V, R\right]$.

Strictly speaking, our analysis applies to the case of a droplet pinned to the substrate at a fixed contact radius *R*. Practically however, Eq. 1 also captures the stability limit of droplets constrained by a constant contact angle θ with a substrate. Provided there exists any miniscule amount of contact angle hysteresis for the droplet on the surface, as is typically the case in practice [36], the appropriate types of variations about the critically stable droplet shape are those at constant *R* because θ may vary infinitesimally within the finite window of contact angles provided by the hysteresis. In this case, Eq. 1 is exact. For example, a droplet subject to an electric field of slowly increasing strength E_0 will progress through a continuum of quasi-static shapes with changing *R* in order to satisfy the constraint on θ, which in this example is the receding contact angle (Fig. 2c, [36]). This may be viewed as changing the absolute scale in accordance with *R* until reaching the limit of stability, at which *R* is constant for variations about the critically stable droplet shape. The relationship between θ and $\frac{\varepsilon E_0^2}{\gamma/R}$ is given in Fig. 2d; these quantities are in fact the two dimensionless groups that may be constructed from the governing parameter set $\left[\gamma, \varepsilon E_0^2, \theta, R\right]$.

The critically stable droplet shape for $\theta = \pi/2$ is a special case because the surface of the droplet together with the surface of the metal plate define an equipotential surface corresponding to half of a free floating droplet in the uniform field E_0. Previous experiments performed for this special case used centimetric soap bubbles placed between parallel plate electrodes, and were performed by slowly increasing E_0 until the stability limit was reached as described in Fig. 2c; the results coincide with Eq. 1 (Fig. 2b(i,ii)) [7,24]. G.I. Taylor's calculation [1], which re-expressed in our parameters yields $\frac{\varepsilon E_0^2}{\gamma/R} = 0.170$ and $\frac{R^3}{V} = 0.251$, coincides with the square indicated by (i) in Fig. 2b.

In summary, we find that a single power law (Eq. 1) captures the electrical stability limit for any finite conductivity droplet (e.g., any aqueous or ionic solution) on timescales greater than its electrical relaxation time. The radius of the droplet may range from ~1 mm, above which gravitational forces become significant, to ~100 nm or smaller, below which charge screening lengths and Van der Waals forces are significant [37]. The power law can aid in understanding natural and engineered systems, and provides a practical design criterion for application development. For instance, the performance of industrial-scale electrospinning [38], electrostatic filtration [13], demulsification [39], and condensation-driven thermal systems [40] often relies on the design of surfaces that carefully manage the supply and electrostatic stability of droplet arrays or liquid films.

References and Notes:

[1] G. Taylor, Proc. R. Soc. London A **280**, 383 (1964).

[2] R. T. Collins, J. J. Jones, M. T. Harris, and O. a. Basaran, Nat. Phys. **4**, 149 (2008).

[3] J. Zeleny, Phys. Rev. **10**, 1 (1917).

[4] J. Zeleny, Phys. Rev. **3**, 69 (1914).

[5] C. T. R. Wilson, Philos. Trans. R. Soc. London. Ser. A. Contain. Pap. a Math. or Phys. Character **221**, 73 (1921).

[6] C. T. R. Wilson, Proc. R. Soc. A **236**, (1956).

[7] C. T. R Wilson and G. I. Taylor, Math. Proc. Cambridge Philos. Soc. **22**, 728 (1925).

[8] C. G. Garton and Z. Krasucki, Proc. R. Soc. A Math. Phys. Eng. Sci. **280**, 211 (1964).

[9] M. Cloupeau and B. Prunet-Foch, J. Electrostat. **25**, 165 (1990).

[10] J.-U. Park, M. Hardy, S. J. Kang, K. Barton, K. Adair, D. kishore Mukhopadhyay, C. Y. Lee, M. S. Strano, A. G. Alleyne, J. G. Georgiadis, P. M. Ferreira, and J. A. Rogers, Nat. Mater. **6**, 782 (2007).

[11] J. B. Fenn, M. Mann, C. K. Meng, S. F. Wong, and C. M. Whitehouse, Science **246**, 64 (1989).

[12] V. E. Krohn and G. R. Ringo, Appl. Phys. Lett. **27**, 479 (1975).

[13] A. Jaworek, A. Krupa, A. T. Sobczyk, A. Marchewicz, M. Szudyga, T. Antes, W. Balachandran, F. Di Natale, and C. Carotenuto, J. Electrostat. **71**, 345 (2013).

[14] V. Gamero-Castano, M., Hruby, J. Propuls. Power **17**, 977 (2001).

[15] Y. M. Shin, M. M. Hohman, M. P. Brenner, and G. C. Rutledge, Polymer (Guildf). **42**,

9955 (2001).

[16] X.-H. Qin and S.-Y. Wang, J. Appl. Polym. Sci. **102**, 1285 (2006).

[17] J. Visser, F. P. W. Melchels, J. E. Jeon, E. M. van Bussel, L. S. Kimpton, H. M. Byrne, W. J. A. Dhert, P. D. Dalton, D. W. Hutmacher, and J. Malda, Nat. Commun. **6**, 6933 (2015).

[18] A. C. Wang, C. Wu, D. Pisignano, Z. L. Wang, and L. Persano, J. Appl. Polym. Sci. **135**, 45674 (2018).

[19] Q. P. Pham, U. Sharma, and A. G. Mikos, Tissue Eng. **12**, 1197 (2006).

[20] K. Kataria, A. Gupta, G. Rath, R. B. Mathur, and S. R. Dhakate, Int. J. Pharm. **469**, 102 (2014).

[21] A. R. Abate, T. Hung, P. Mary, J. J. Agresti, and D. A. Weitz, Proc. Natl. Acad. Sci. U. S. A. **107**, 19163 (2010).

[22] J. S. Eow and M. Ghadiri, Chem. Eng. J. **85**, 357 (2002).

[23] O. A. Basaran and L. E. Scriven, Phys. Fluids A Fluid Dyn. **1**, (1989).

[24] O. A. Basaran and L. E. Scriven, J. Colloid Interface Sci. **140**, 10 (1990).

[25] H. J. Cho, I. S. Kang, Y. C. Kweon, and M. H. Kim, Int. J. Multiph. Flow **22**, 909 (1996).

[26] M. T. Harris and O. A. Basaran, J. Colloid Interface Sci. **161**, 389 (1993).

[27] A. R. Padday, J. F., Pitt, Philos. Trans. R. Soc. LONDON A. Math. Phys. Sci. **275**, 489 (1973).

[28] R. A. Brown and L. E. Scriven, Proc. R. Soc. A Math. Phys. Eng. Sci. **371**, 331 (1980).

[29] R. Courant and D. Hilbert, *Methods of Mathematical Physics. Vol. 1* (Wiley, 1989).

[30] We found that a separation distance $S \gtrsim 3V^{1/3}$ is sufficient for the position of the second plate to negligibly influence the experiment measurements.

[31] J. R. Melcher, G. I. Taylor, T. R. Melcher, and G. I. Taylor, Annu. Rev. Fluid Mech. **1**, 111 (1969).

[32] This upper limit on R is evident through $\frac{\varepsilon E_0^2}{\gamma/R}$ and $\rho g V^{2/3}/\gamma$ having respective linear and quadratic dependencies on the absolute scale of the experiment.

[33] G. I. Barenblatt, *Scaling, Self-Similarity, and Intermediate Asymptotics* (Cambridge University Press, 1996).

[34] S. B. Sample and C. D. Hendricks, Int. J. Eng. Sci. **7**, 427 (1969).

[35] J. D. Jackson, *Classical Electrodynamics*, 3rd ed. (Wiley, 1999).

[36] D. Quéré, Annu. Rev. Mater. Res. **38**, 71 (2008).

[37] J. Israelachili, *Intermolecular and Surface Forces*, 3rd ed. (Elsevier Inc., 2011).

[38] O. Akampumuza, H. Gao, H. Zhang, D. Wu, and X.-H. Qin, Macromol. Mater. Eng. **303**, 1700269 (2018).

[39] S. Mhatre, V. Vivacqua, M. Ghadiri, A. M. Abdullah, M. J. Al-Marri, A. Hassanpour, B. Hewakandamby, B. Azzopardi, and B. Kermani, Chem. Eng. Res. Des. **96**, 177 (2015).

[40] S. Rashidi, H. Bafekr, R. Masoodi, and E. M. Languri, J. Electrostat. **90**, 1 (2017).

Acknowledgements: Data points are tabulated in the Supplementary Materials. Financial support was provided by grants from the MIT Deshpande Center for Technological Innovation, the Assistant Secretary of Defense for Research and Engineering (Air Force Contract No. FA8721-05-C-0002) via MIT Lincoln Laboratory, a National Science Foundation CAREER Award to A.J.H. (CMMI-1346638), a National Science Foundation grant to J.W.M.B. (CMMI-1727565), and a Department of Defense Science and Engineering Graduate Fellowship Award to J.B.

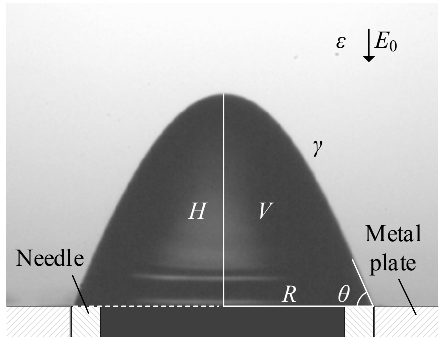

FIG. 1. Experimental setup for determining the stability limit of soap-water droplets on a conducting surface subject to a uniform electric field E_0 in a dielectric medium ε. The droplet has surface tension γ and is pinned to the outer radius R of a metal needle tip coincident with the surface of a metal plate. Liquid is slowly dispensed into the droplet until it becomes unstable. The camera frame capturing the critically stable droplet shape (as shown here) is image processed to calculate its volume V, height H, and contact angle θ.

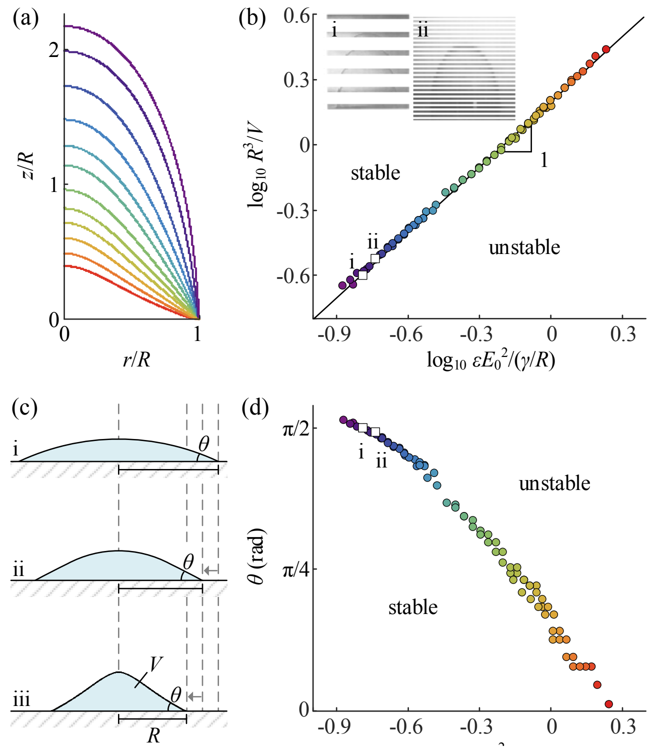

FIG. 2. Experiment results for the critically stable droplets. (a) The critically stable droplet shapes constitute a continuous family where each is non-elementary and non-similar to any other. (b) A power law relating the dimensionless groups characterizes the stability limit of the droplets. The black line is Eq. 1. The square data points and corresponding inset pictures are for critically stable soap bubbles on a metal plate exposed to a uniform field from experiments performed in (i) 1925 [7] and repeated in (ii) 1990 [24]. (c) A droplet constrained to slide on a surface with constant contact angle θ progresses through the following sequence for a slowly increasing electric field E_0: (i) for $E_0 = 0$, the droplet shape is a spherical cap; (ii) as E_0 increases, the droplet deforms and contracts its contact radius R; (iii) At the limit of stability, the critically stable droplet parameters are again captured by Eq. 1. (d) For each critically stable droplet shape, there is a unique corresponding contact angle θ.